Chapter 4

Designing Mu Robust Controller in Wind Turbine in Cold Weather Conditions

Tahere Pourseif, Majid Taheri Andani,
Hamed Pourgharibshahi, Hassan Zeynali and
Arash Shams

Additional information is available at the end of the chapter

http://dx.doi.org/10.5772/intechopen.74626

Abstract

Due to wind turbine is in class of complex nonlinear system so the precise model of this plant is not accessible, therefore it can be categorized as an uncertain model. So, controlling of this system is a demanding topic. Many of schemes which presented for controlling of wind turbines investigate these systems in a good weather condition. However, many turbines work in severe weather condition. In this study, wind turbine is suggested in cold weather, and in ice on turbine blades which they are considered as uncertainties in the model. A robust controller is designed for the wind turbine, to control the pitch angle.

Keywords: ice formation on wind turbine blades, robust mu control, uncertainty, wind turbine

1. Introduction

The growth of the population in world causes to increase of electrical power consumption. Overpopulation also leads to depletion of fossil fuel energy, degradation of environment. These consequences motivate scholars to seeking better ways to produce electrical power [1, 2]. Therefore, alternative energies where their sources are Renewable can be an effective alternative way to produce electricity that generate from natural processes that can be refilled continually and are unpredictable. Therefore, the control of this kind of energy is challengeable. The renewable energy is practical because of its being low-priced, easily accessible, and purity of the energy. Wind turbine is a tool which is operates on a noncomplex principle that transforms the kinetic energy of wind into electrical energy. Various control methods are presented to regulate the wind turbine speed for effective power generation and to maintain the turbine elements within designed speed and torque bounds [1, 3]. In [4] performance of the turbine for working in various operation is investigated and for operating in the third are a controller is designed. In [5], a well-known robust controller which is named as sliding mode controller is utilized to control power as well as to adjust wind's rotor speed and turbine generator. Due to exist the nonlinear in the characteristics of the controller, just two uncertainties such as spring constant and damping coefficient have been considered and employed to the wind turbine system. The main problem of this scheme is the chattering that produce by Sliding mode controller on control actions in [6], another robust controller is proposed to view all of the uncertainties. These uncertainties comprise the uncertainty is produced from the linearization procedure and minor deviations, and from damping coefficient and spring constant. These approaches are applied to control the pitch angle and enlarge electrical power generation [7]. In many cases, the perfuming of the wind turbine is examined in appropriate weather conditions. But, a robust controller is designed in this paper to keep the performing of the wind turbine in a severe weather conditions, like snow or in a situation that rain droplets freeze on the turbine blades [8]. In these scenarios, when the turbine blades freeze, the mass of the rotor would be changed and the electric power decreases. Then, the controller is given to regulate the speed of the generator after employing the uncertainties in the inertia and other factors [9, 10]. In light of the pitch angle and the speed of the rotor the kind of wind turbine applied in this research has different rotor speed and different pitch angle. The regulation of the changeable pitch angle and the changing rotor speed, respectively, lead to increasing of the electrical power and decreasing of the dynamic load of the turbine. It should be mentioned that that the modification of the variable rotor speed not only minimizes the turbine's dynamic load, but also increases the system's lifespan [11, 12]. The aim of designing the controller is to maximize the electrical power production at low wind speed and to keep it at high wind speed. In comparison with other publications that have done on wind turbine, it is the first time which the uncertainty that arises from icing of wind blade is considered, and for this condition then robust controller is proposed.

2. Wind turbine model

2.1. Wind turbine

Effective wind speed is a nonlinear stochastic process that is approximated by a linear model in order to simplify and satisfy the control objectives [9]. There are two terms in the wind model:

$$V = V_t + V_m \tag{1}$$

In this model the wind has two elements, mean value term (V_m) and turbulent term (V_t).

In which:

$$V_m = \frac{1}{T}\int_{t-\frac{T}{2}}^{t+\frac{T}{2}} v(\tau)\, d\tau \tag{2}$$

http://dx.doi.org/10.5772/intechopen.74626

$$V_t = \frac{k}{(p_1 s + 1)(p_2 s + 1)} e; e \in N(1, 0) \tag{3}$$

The turbulent term V_t can be modeled by:

$$\begin{pmatrix} \dot{V}_t \\ \ddot{V}_t \end{pmatrix} = \begin{bmatrix} 0 & 1 \\ -\frac{1}{p_1 p_2} & -\frac{p_1 + p_2}{p_1 p_2} \end{bmatrix} \begin{pmatrix} V_t \\ \dot{V}_t \end{pmatrix} + \begin{bmatrix} 0 \\ \frac{k}{p_1 p_2} \end{bmatrix} v \tag{4}$$

where, $v \in N(1, 0)$ and the parameters p_1, p_2 and k depend on the mean value of the wind speed (V_m).

2.2. Nonlinear model of wind turbine system

In this section, for deriving the model, the entire wind turbine is separated into four subsystems: aerodynamics subsystem, mechanical subsystem, generator subsystem and pitch actuator subsystem. The aerodynamic subsystem transforms wind forces into mechanical torque and thrust on the rotor. The mechanical subsystem contains of the drivetrain, tower and blades. The drivetrain converts torque of the rotor to the electrical generator. The tower keeps the nacelle and resists the thrust force and the blades transform wind forces into the aerodynamics torque and thrust. The generator subsystem transforms mechanical energy to electrical energy and finally the blade-pitch and generator-torque actuator subsystems are portion of the control model. To model the overall wind turbine, models of these subsystems are attained and at the end they are linked together. A wind model is attained and increased with the wind turbine model to be considered for wind speed estimation. **Figure 1** shows the basic subsystems and their interactions.

Numerous degrees of freedom can be used to model the plant, but for control design mostly just a less important degrees of freedom are used. In this study we just use two degrees of freedom, namely the rotational degree of freedom (DOF) and drivetrain torsion. The subsystems nonlinear model of wind turbine is used in the following:

2.2.1. *Aerodynamics subsystem*

The following nonlinear equation is the model of the aerodynamics subsystem [13]:

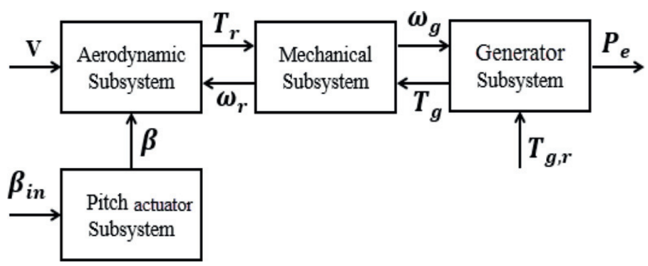

Figure 1. Schematic of the wind turbine.

$$P_r = \frac{1}{2}\rho\pi R^2 V^2 C_p(\lambda, \beta) \tag{5}$$

Where, P_r is the electrical power of rotor, ρ is the density of wind ($\frac{Kg}{m^3}$), R is the radius of the blades (m), V is the wind speed (m/s), λ is the tip speed ratio, β is the pitch angle, C_p the power coefficient, λ is the ratio between the blade tip speed and the wind speed:

$$\lambda = \frac{V}{R\omega_r} \tag{6}$$

where the ω_r is the angular speed of rotor. The derivative of C_p with respect to both λ and β are therefore used extensively in the control designs. In previous work, numerical derivatives of C_p with respect to λ and θ have been successfully obtained and utilize in linear control designs. However, the nonlinear controllers have proven sensitive towards the noise introduced by the numerical derivations, making it difficult to validate the responses obtained by e.g. a feedback linearizing controller. Consequently, it has been Chosen to base the aerodynamic model on an analytic expression of C_p. The relation between C_p, β and λ can be written as [13]:

$$C_p(\lambda, \beta) = 0.22\left(\frac{116}{\lambda_t} - 0.6\beta - 5\right)\exp\left(\frac{12.5}{\lambda_t}\right) \tag{7}$$

where,

$$\frac{1}{\lambda_t} = \frac{1}{\lambda^{-1} + 0.12\beta} - \frac{0.035}{(1.5\beta)^2 + 1} \tag{8}$$

2.2.2. Generator subsystem

The synchronous generator is supposed to be idea, so the power of generator is calculated in [14]:

$$P_e = T_g\omega_g \tag{9}$$

The P_e denoted electrical power of generator, the generator's angular speed is shown by ω_g and the T_g represents generator torque which is controllable, although, it is not practical to change immediately. The response of generator's dynamic is modeled with a first order linear model [6]:

$$\dot{T}_g = -\frac{1}{\tau_T}T_g + \frac{1}{\tau_T}T_{g,r} \tag{10}$$

where $T_{g,r}$ represents the generator torque reference value and the time constant is denoted by τ_T

2.2.3. Pitch actuator subsystem

The blade's pitch begins to change by a hydraulic/mechanical actuator to push the angle of blade β to tracks the reference of blade angle β_{in}, The pitch of the blades is changed by a hydraulic/mechanical actuator Eq. (11) is a first order linear model which is a simplified of the dynamic model [6]:

$$\dot{\beta} = -\frac{1}{\tau_\beta}\beta + \frac{1}{\tau_\beta}\beta_{in} \tag{11}$$

where τ_β is the time constant.

2.2.4. Mechanical Subsystem

Figure 2 shows a schematic of the wind turbine mechanics. The turbine is split into two parts, separated by the transmission: The rotor side and the generator side [15].

J_r denotes the inertia which is on the rotor side and generator side is represented by J_g which is on the leftmost and the rightmost disc respectively. The shaft link the rotor to the transmission is subject to huge torques that leads it to twist, so the shaft is suitably modeled as a damped spring. T_r, which denotes rotor torque, excites the model on the left T_g that represents the generator torque excites the model on the right. The torques and T_{sg} are the torques at each side of the transmission part and has relation by N_g represents the gear ratio which is a relation between T_{sr} and T_{sg} that are named the torque of each side of the transmission part.

$$T_{sg} = \frac{T_{sr}}{N_g} \tag{12}$$

The equations describing the dynamics are obtained using Newton's second law for rotating bodies. This results in two equations: one for the rotor side and one for the generator side.

$$\dot{\omega}_r = T_r - T_{sr} \tag{13}$$

$$\dot{\omega}_g = T_g - T_{sg} \tag{14}$$

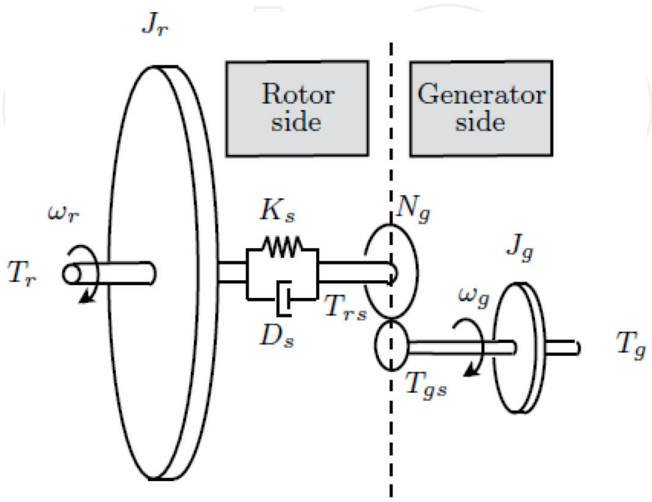

Figure 2. Schematic of the wind turbine mechanics.

Introducing a variable δ [rad] describing the twist of the shaft, leads to the following equation describing the twist of the flexible shaft [16]:

$$T_{sr} = D_r\dot{\delta} + K_r\delta \tag{15}$$

where:

$$\delta = \Omega_r - \frac{\Omega_g}{N_g},\ \dot{\delta} = \omega_r - \frac{\omega_g}{N_g} \tag{16}$$

In the above equations, D_r represents the damping and K_r denotes spring coefficient, angular speed of rotor is defined by ω_r, the angular speed of generator represent by ω_g, Ω_r and Ω_g are used to define the default shaft angle at the rotor and the default shaft angle at the generator, respectively.

2.3. Linearized models of wind turbine system

As it was discussed in previous section, for design a controller a linear model of the system is needed. The input of this model is wind [17]:

$$input = \begin{bmatrix} V & \beta_{in} & T_{g,r} \end{bmatrix}^T \tag{17}$$

And outputs of the system include:

$$output = \begin{bmatrix} \omega_r & \omega_g & P_e \end{bmatrix} \tag{18}$$

Having all the equations, system equations become: [8]:

$$\dot{\omega}_r = \frac{a - D_r}{J_r}\omega_r - \frac{a - D_r}{J_r N_g}\omega_g - \frac{K_r}{J_r}\delta + a_{14}\beta \tag{19}$$

$$\dot{\omega}_g = \frac{D_r}{N_g J_g}\omega_r - \frac{D_r}{{N_g}^2 J_g}\omega_g + \frac{K_r}{J_g N_g}\delta - \frac{1}{J_g}T_g \tag{20}$$

$$\dot{\delta} = \omega_r - \frac{\omega_g}{N_g} \tag{21}$$

$$\dot{\beta} = -\frac{1}{\tau_\beta}\beta + \frac{1}{\tau_\beta}\beta_{in} \tag{22}$$

$$\dot{T}_g = -\frac{1}{\tau_T}T_g + \frac{1}{\tau_T}T_{g,r} \tag{23}$$

$$\dot{V}_t = V_t \tag{24}$$

$$\ddot{V}_t = -\frac{1}{p_1 p_2}V_t - \frac{p_1 + p_2}{p_1 p_2}\dot{V}_t + \frac{k}{p_1 p_2}v \tag{25}$$

http://dx.doi.org/10.5772/intechopen.74626

In which J_r and J_g are rotor and generator moments of inertia, τ_β and τ_T are time constants of the first order actuator models

3. Uncertainties model

Various uncertainties have been examined in the current literature. These uncertainties derive from approximated and process parameters in a nonlinear system which changes as the operating point changes, a matter causing the electrical power production to reduce. There are always discrepancies between real system and mathematical models, which lead to uncertain models. In this work, sources of uncertainties are taken to be:

- Uncertainty in the drivetrain stiffness and damping parameters.
- Uncertainty in the linearized model.

Although, all control design presented design for moderate temperature. Decreasing the temperature in winter has devastating properties on the wind turbine. Ice on the elements of wind turbine leads some serious problems. Even a few amount of ice on the blades worsens the aerodynamic performance of the wind turbine. It not only decreases the output power energy, but also raises the abrasion between the elements [11, 16]. In other word, the ice in cold places and the high density of air at cold climate have damaging properties on aerodynamics. Fluctuation of produced power and load are reason for such dysfunctionality. Masses of the ice on the turbine cause fluctuation on the frequency of the turbine's elements and also the behavior of the system's dynamic [10–12]. In addition, this condition has effect on control plant. In other word, the performance of the turbine system worsens through wrong data sending [11]. Previous article dealing with this issue have presented approaches like observation, the use of sensors and monitors, considering aerodynamic sound, etc., to recognize ice. The control schemes are then designed to eliminate the ice [9, 10, 17].

3.1. The impact of cold weather on the operation of wind turbine

In this research, for the first time a new approach is advanced to enhance the wind turbine performance in cold climate conditions and to stop the damage which cause about the shutdown of the turbine. Because of the structure of the wind turbine, when frozen blades' masses changes, the rotor mass will be changed and lead to the inertia of rotor. These variations will effect on equations of the wind turbine and optimal power creation. Therefore, control of turbine and optimal power output could be possible by considering the inertia of the rotor as a new component of uncertainty in the plant. The value of this uncertainty differs with decreasing the temperature and the turbine's production capacity. In [18], imbalance of the blade was simulated by scaling the density of mass of one blade, which generates an imbalance distribution of mass with respect to the rotor. Furthermore, the aerodynamic asymmetry was simulated by adjusting the pitch of one blade, which produces an imbalance torque across the rotor. In our work, the blade imbalance in blade is due to icing on the blade. Thus, the uneven of the blade is considered about 20% as uncertainty. A robust control is designed to control the turbine in the existence of uncertainty because of the blade imbalance icing [19]. The uncertainties in the wind turbine comprise the linearized model parameters which is extracted from the nonlinear plant, spring constant, and damping coefficient that alteration as the working point diverges; another uncertainty which is added to the system because of the presence of noise and disturbance in the input signal. All of these uncertainties are considered in appropriate weather conditions. In this work, cold climate condition and inertia of rotor are considered as other sources of uncertainty in the wind turbine system [20, 21].

3.2. Frequency response of wind turbine

These icy turbine blades change the rotor mass. Under the frequency response analysis of the system is shown in **Figure 3**, the rotor inertia uncertainty can be considered between the range of 0 and 20% and The Wind turbine system is stability:

According to, the red color is nominal frequency response and blue color is system uncertainties that uncertainty is considered between the range of 0–20%. The system has positive phase margin and positive gain margin, so it is stable.

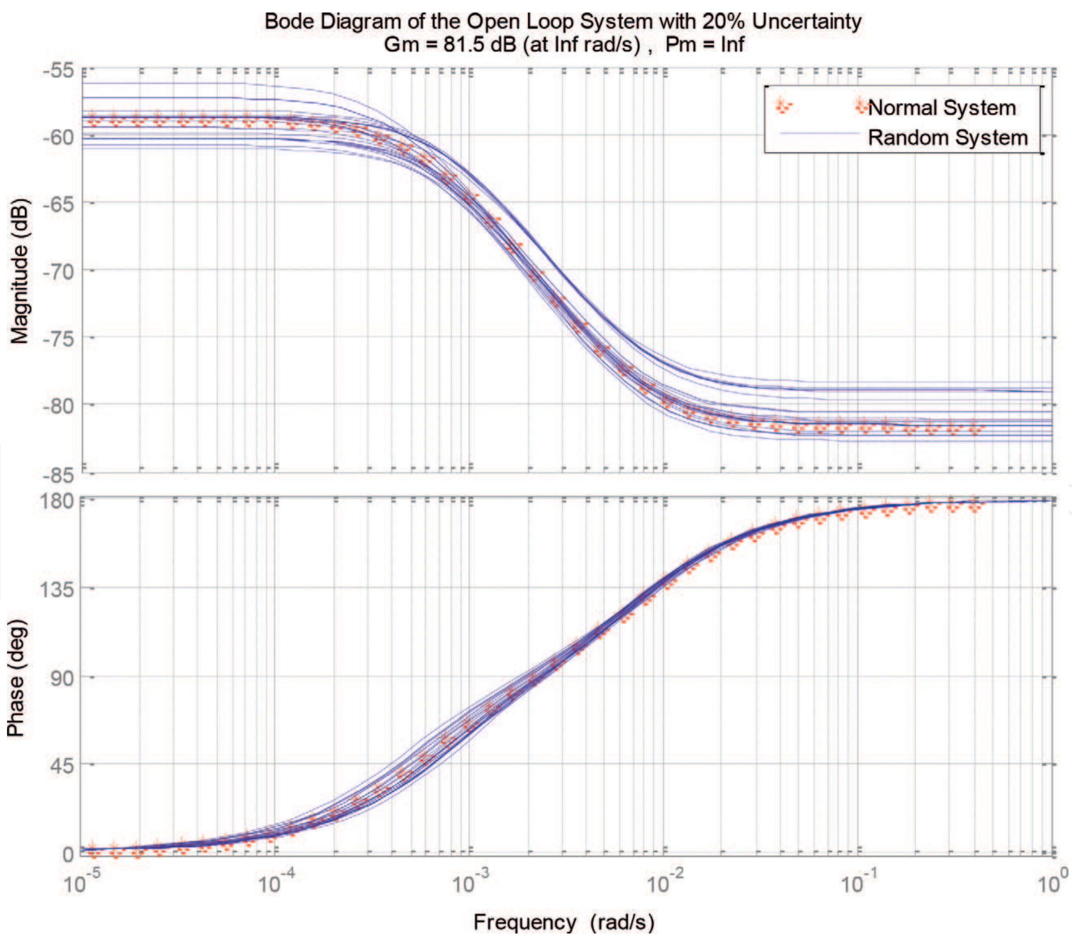

Figure 3. Bode diagram open loop system with 20% uncertainty of inertia rotor.

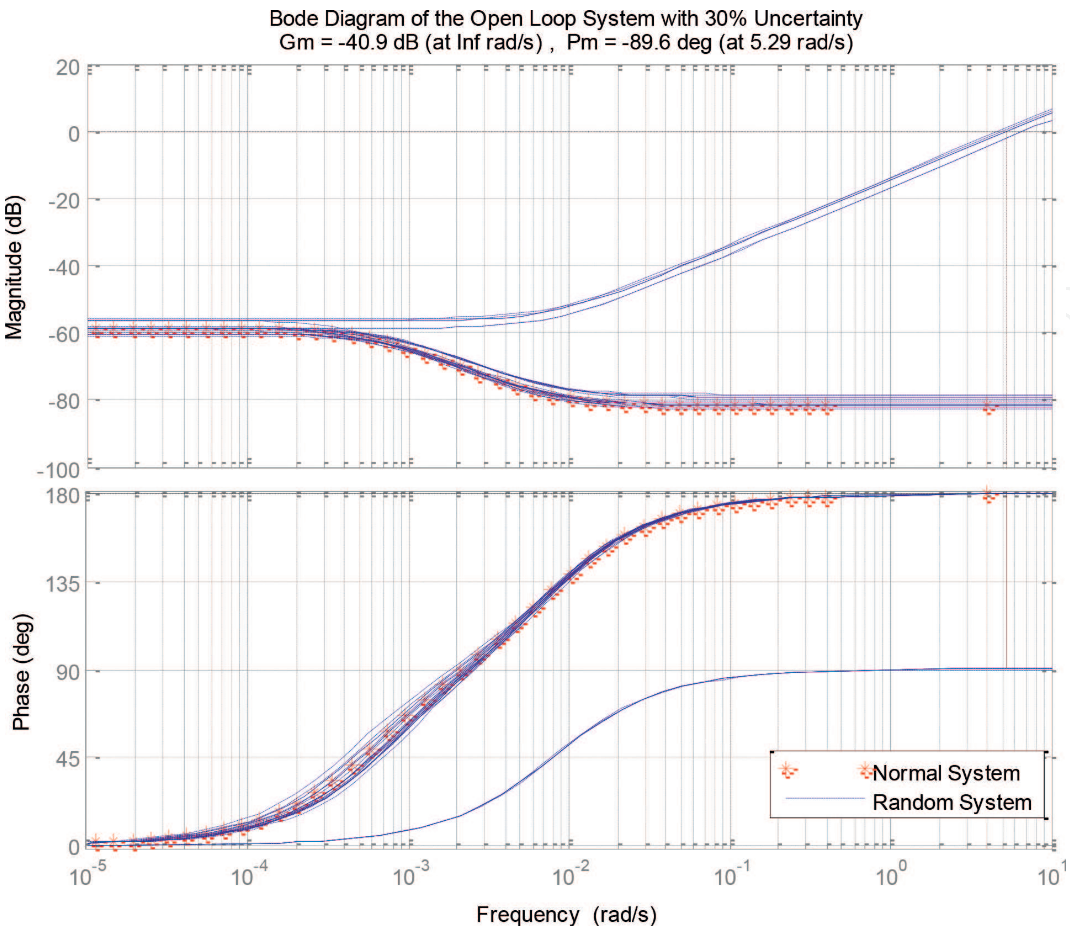

Figure 4. Bode diagram open loop system with 30% uncertainty of inertia rotor.

Figure 4 shows that the system is unstable by considering range of uncertainty between 20 and 30%. So system uncertainties are defined between 0 and 20%.

The uncertainties in parameters can be shown as follows:

$$K_r = \overline{K}_r\left(1 + p_{K_r}\delta_{K_r}\right) \tag{26}$$

$$D_r = \overline{D}_r\left(1 + p_{D_r}\delta_{D_r}\right) \tag{27}$$

$$a = \overline{a}(1 + p_a\delta_a) \tag{28}$$

$$a_{14} = \overline{a}_{14}\left(1 + p_{a_{14}}\delta_{a_{14}}\right) \tag{29}$$

$$J_r = \overline{J}_r\left(1 + p_{J_r}\delta_{J_r}\right) \tag{30}$$

Two reasons exist which explain that spring coefficient and the damping can be considered as uncertainties. One reason is, there exist divergence in the spring variables from fabrication to fabrication, and manufacturer to manufacturer and other reason, it should be consider that the

Parameter	Description	Unit	Tolerance
K_r	spring coefficient	Nm/rad	±10%
D_r	Damping	$\left(\frac{kg.m^2}{rad.s}\right)$	±10%
A	Linearization parameter	—	±20%
a_{14}	Linearization parameter	—	±20%
J_r	rotor inertia	$kg.m^2$	+20%

Table 1. Parameter uncertainties of the wind turbine.

spring parameter and damping can be changed during a long time because of continuous working, and aging. In previous equations, $\overline{K}_r$, $\overline{D}_r$, $\overline{a}$, $\overline{a}_{14}$ are nominal parameter values, resulting from the spring constant, damping coefficient, linearization process and rotor inertia, respectively. p_{K_r}, p_{D_r}, p_{a}, $p_{a_{14}}$ indicate maximum relative uncertainties that are for uncertainty parameters shown in **Table 1**.

δ_{K_r}, δ_{D_r}, δ_{a}, $\delta_{a_{14}}$ and δ_{J_r} are relative changes in these parameters. Therefore:

$$|\delta_{K_r}| \le 1, |\delta_{D_r}| \le 1, |\delta_a| \le 1, |\delta_{a_{14}}| \le 1, |\delta_{J_r}| \le 1 \tag{31}$$

4. Robust design controller

4.1. Closed loop system design specifications

Figure 5 shows the block diagram of Wind turbine closed loop system, including the feedback structure, the controller, as well as the model uncertainties and performance objectives weights.

In **Figure 5**, (r) shows the reference input, (V) represents the wind speed which has disturbance, (n) denotes noise and e_u and e_y are considered as two output costs. The system (R)

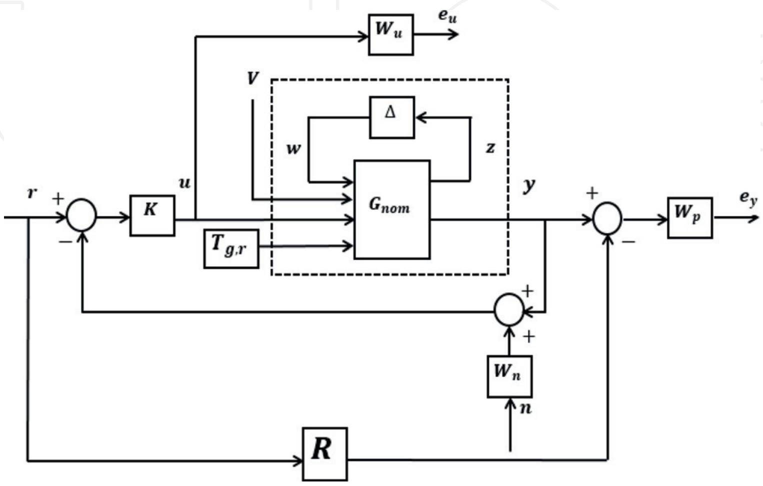

Figure 5. Block diagram of the closed-loop system with performance specifications [22].

represents the performance when model is ideal, to which the designed closed-loop system wants to reach [23]. The transfer function of model is chosen in a way that the time response of the reference signal has an overshoot less than around 5%. Inside the dots rectangle is the ideal model, which shows with, G_{nom} of the wind turbine model and the block Δ that parameterizes uncertainties in the model. To find the wanted performance, inputs r can be obtained from the transfer function matrix, and we need to find disturbance in V and also n to outputs e_u and e_y. Thus the infinity norm of that transfers function can be minor for the entire existing uncertainty variable. The position noise signal is attained by moving the unit-bounded signal which is shows by n through the weighting transfer matrix which denotes W_n. The transfer matrices W_p and W_u represent the relative significance of the diverse frequency spans for which the performance is needed. So, the performance aim can be reorganize, with probable slight conservativeness, like that transfer function matrix infinity norm be less than 1. So Δ matrix is given in following form:

$$\Delta = \mathrm{diag}\left(p_{K_r}, p_{D_r}, p_a, p_{a_{14}}, p_{J_r}\right) \tag{32}$$

This transfer function can be written as [21]:

$$\begin{bmatrix} e_u \\ e_y \end{bmatrix} = \begin{bmatrix} W_p(\mathrm{S_o G_u K - R}) & W_p \mathrm{S_o G_v} & -W_p \mathrm{S_o G_u} K W_n \\ W_u \mathrm{S_i} K & -W_u K \mathrm{S_o G_v} & -W_u K \mathrm{S_o} W_n \end{bmatrix} \begin{bmatrix} r \\ V \\ n \end{bmatrix} \tag{33}$$

where $S_i = (I + KG)^{-1}$ and $S_o = (I + GK)^{-1}$ are the input and output sensitivities, repectively. Note that S_oG is the transfer function between V and y.

4.1.1. Robust stability

By definition, the closed loop system achieves robust stability if the closed loop system is internally stable for each possible plant dynamics $G = F_u(G_{nom}, \Delta)$.

4.1.2. Robust performance

The closed loop system must remain internally stable for each $G = F_u(G_{nom}, \Delta)$ and in addition the performance criterion should be satisfied for each $G = F_u(G_{nom}, \Delta)$ [21].

4.2. Matching transfer function and weighting transfer functions

In the case of mu controller optimization design, we have to define the model transfer function which is denote with R and the weighting transfer functions that are nominated with W_n, W_p and W_u.

The model transfer function is selected therefore the time response to the reference signal has an overshoot fewer than 50% and a settling time not more than 1 ms. A probable plant which please the requirements is:

$$R(s) = \frac{1}{0.48s^2 + 0.95s + 1} \tag{34}$$

In **Figure 6**, the response of matching model to power electrical input is shown.

The noise shaping function W_n is determined on the basis of the spectral density of the position noise signal. In the given case it is taken as the high-pass filter. In this case output has a noteworthy spectral content more than 500 Hz. For this type of filter, the position noise signal is just 0.95 V in the low-frequency values but it is 1 V in the high-frequency values that matches to a position error of around 5% without width.

$$W_n(s) = 95 \times 10^{-5} \frac{0.1s + 1}{0.001s + 1} \tag{35}$$

So the frequency response is shown in **Figure 7**.

The closed-loop system performance specifications are reflected by the weighting performance function W_p.

$$W_p(s) = 0.95 \frac{2s + 50}{2s + 0.005} \tag{36}$$

Figure 8 shows the frequency response of the inverses of this weighting function.

It is shown that in a selection, the objective is to obtain a minor variance between the system and outputs of the model, and a minor effect of the disturbance on outputs of the system. This will ensure nice tracking of the reference input and minor error because of the low-frequency

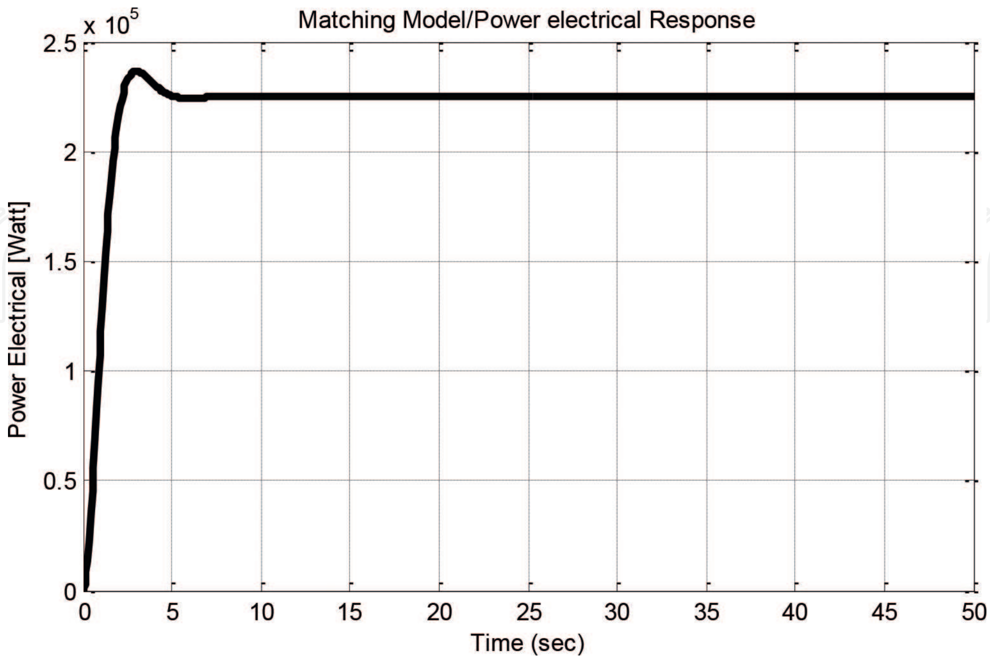

Figure 6. Response of matching model to electrical power input.

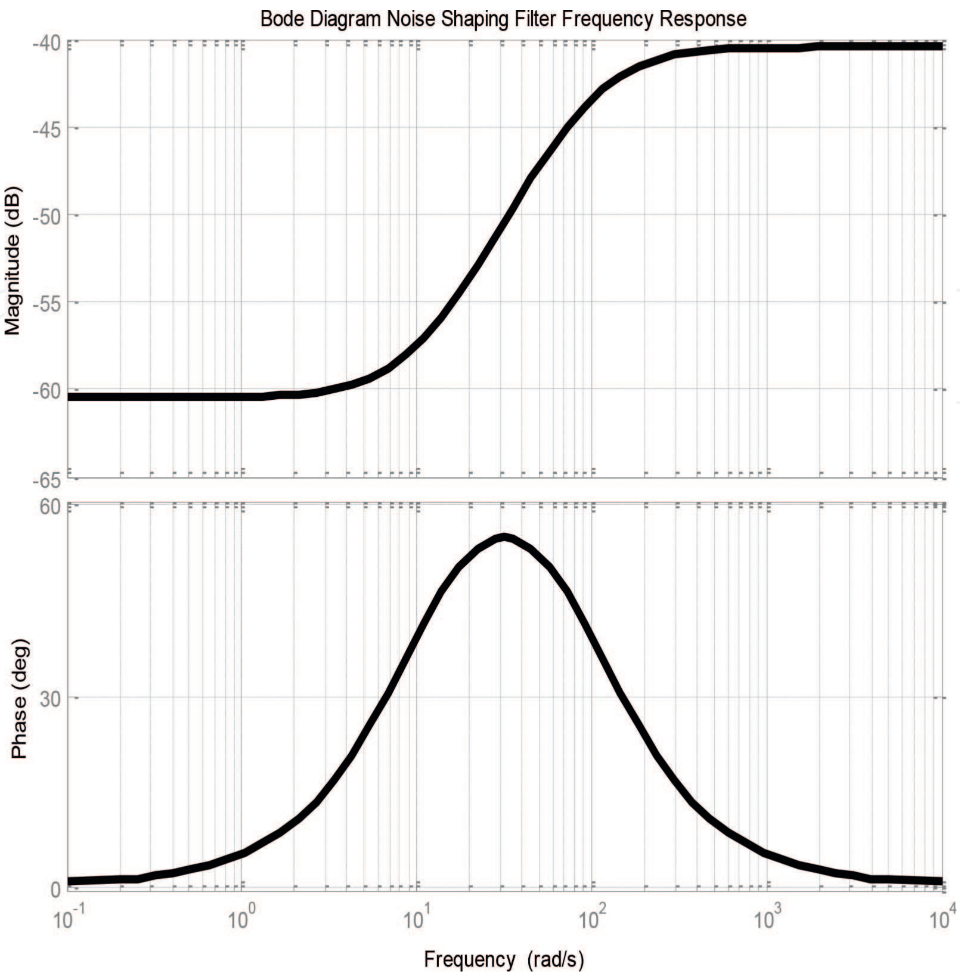

Figure 7. Frequency response of noise filter $W_{n.}$

disturbances. The weight of control function is usually selected as high-pass filters to make sure that the control action will not surpass 25°.

$$W_u(s) = 0.022 \frac{0.8s^2 + 10s + 2}{3.5 \times 10^{-4} s^2 + 20 \times 10^{-2} s + 2} \tag{37}$$

Figure 9 shows the frequency response of this weighting function W_u.

According to the above figure, effort control is very low in low- frequencies that cause reduced the control cost.

4.3. Robust μ controller design

The objective of controller with applying the μ synthesis scheme is the stabilizing of the closed loop of the plant and pleasing all of the control demands. In the existence of measurement noise, disturbance in the wind, and uncertainties, the closed-loop plant should have the robust efficiency. Therefore, the purpose of μ controller scheme is design a controller where the wind

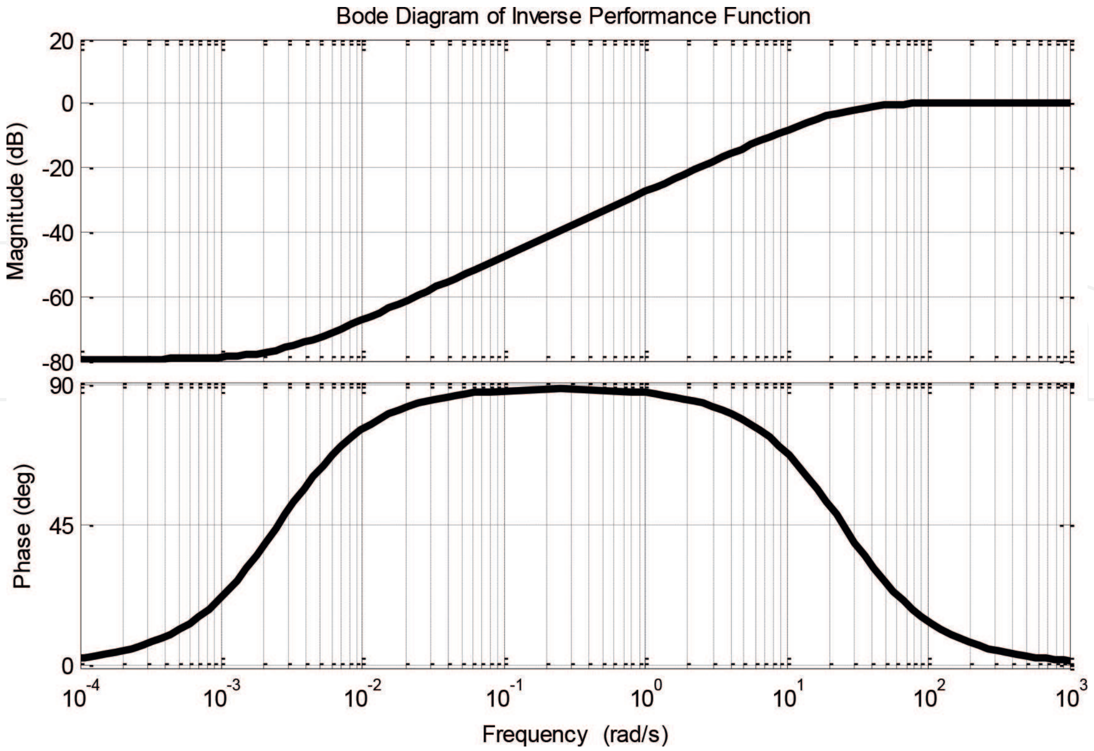

Figure 8. Frequency response of weighting function $\frac{1}{W_P}$.

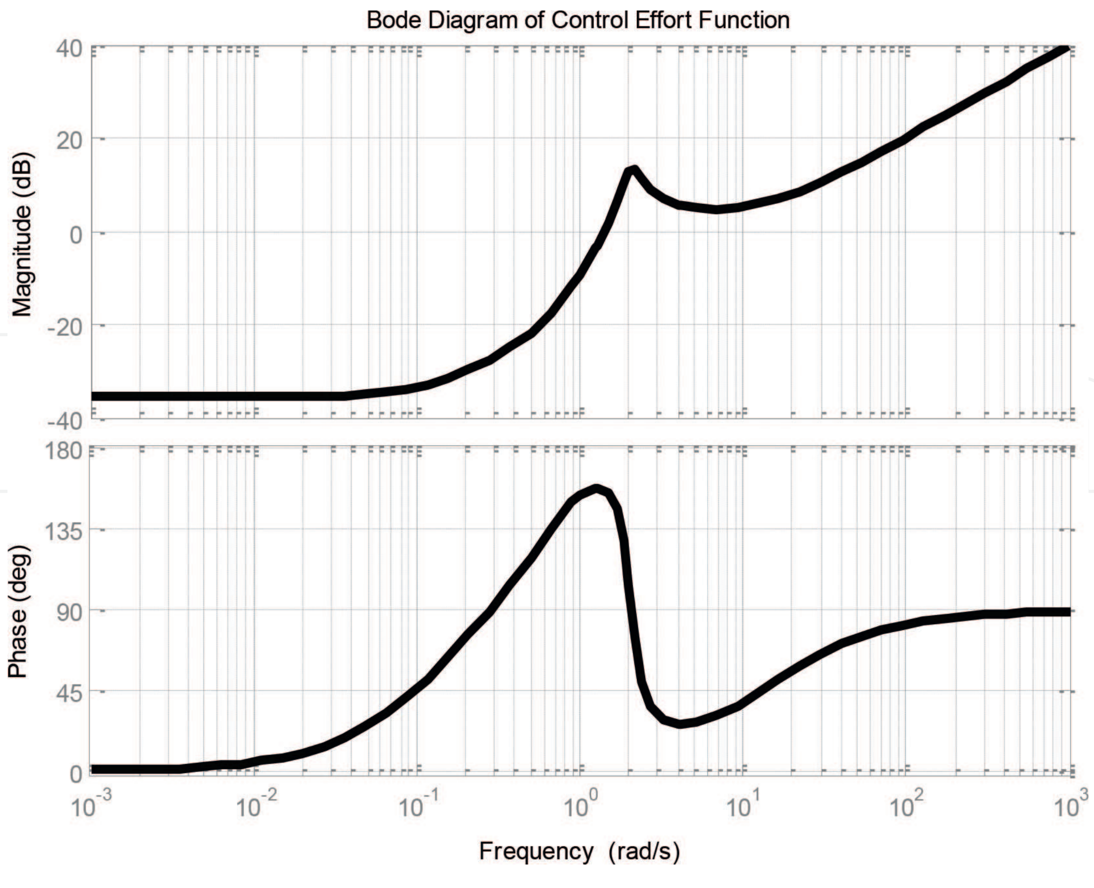

Figure 9. Frequency response of weighting function W_u.

turbine can track the reference input of generated electrical energy when noise and disturbance are exist. In **Figure 10**, the schematic of the closed loop model which is utilized with the defined uncertainties is depicted for μ controller model design.

From the figure, it can be seen that y_c is defined as the difference between noisy output and the reference and the transfer function P(s) shows the open-loop transfer function matrix with 10 inputs and eight outputs. The upper linear fractional transformation (LFT) of the closed loop system is:

$$P = F_u(P_{nom}, \Delta_r) \tag{38}$$

where P_{nom} is the nominal transfer function matrix, Δ_r includes five uncertainties in the wind turbine model. We assume Δ_P is defined the structure of uncertainties block as follows:

$$\Delta_p = \left\{ \begin{bmatrix} \Delta_r & 0 \\ 0 & \Delta_f \end{bmatrix}; \Delta_r \in \mathfrak{R}^{5\times5}, \Delta_f \in C^{4\times2} \right\} \tag{39}$$

Controller, which is attained with this scheme, is typically of high order controller that cause to challenges in a real-world implementation. So for this purpose, it is recommended to decrease the order of the control plant until it is feasible to simplify the closed loop scheme theory and operation. The results of the singular parameter of planned after repeating five iterations of D-K procedure are demonstrated in **Table 2**.

It can be seen that the maximum value of μ is 11.648 that is achieved in the first iteration. Similar to this method, next steps are done to finally value of γ is less than 1. The designed μ controller synthesis is of order 17, and it is achieved after five iterations. In the final iteration, the value of γ is reached to 0.732 and, μ reaches to 0.730 that is less than 1. In other word, the closed-loop scheme has robust performance due to the structured singular parameter is less

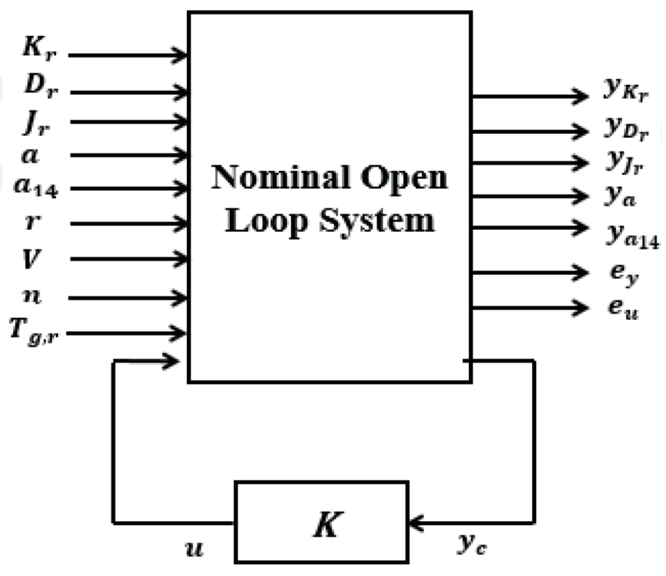

Figure 10. Closed loop system model for design μ robust controller.

Iteration number	γ value achieved	Maximum μ value	Controller order
1	1201.403	11.648	5
2	5.35	3.837	11
3	1.763	0.748	16
4	0.734	0.733	17
5	0.732	0.730	17

Table 2. Obtained results of the robust controller (μ).

than 1 in any frequency. Also, the gamma parameter denotes the value that the function $F_l(P, K)$ infinity norm is fewer than that value.

5. Simulation results of the designed robust controller

The considered wind model in this paper is as follows.

Figure 11 depicts the speed of the wind in the third operating area that is a value between 15 and 25 m/s. In this study, the model of the wind has randomly varies from 15 to 24 m/s In our research, the speed of the wind is considered be highly changeable during the times [8, 9]. As in early times the speed of wind turbine is growing, then its parameter is constant in time and its value fell in the end of the period of the time. The reason for selecting this kind of plant of the random wind is, presentation the robust controller has a good performance in various

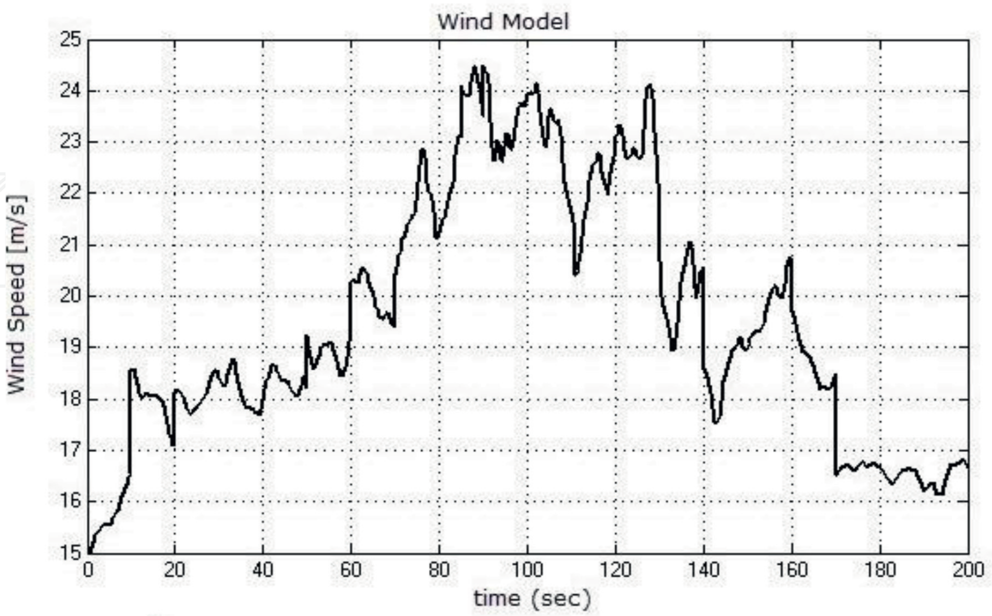

Figure 11. Wind model in different speeds.

http://dx.doi.org/10.5772/intechopen.74626

speeds. This express that a sudden variation in the wind speed, the robust controller attempts to control the pitch angle for setting the electrical power at it's at most efficiency in the third performance area.

Due to the linear dependency among the speed of the rotor and the speed of generator over the gear ratio, the results of applying the control scheme which seeks to maintain the electrical power fixed and regulate speed of the generator- can be examined after modeling of speed of the wind turbine and modeling the robust μ controller.

Considering **Figure 12(a)**, the deflection of output about the nominal value which is changed by noise and disturbance in wind is not high that is acceptable. Maximum variation around the reference value is 2.1% and it is equal to 0.027 kW that expresses nice disturbance cancelation in areas in the matching scheme. In **Figure 12(b)**, at most variations around nominal values are equivalent to 3.068 rad/s and it is equal to 9.2%. It is sates a disturbance cancelation and nice following of generator reference parameter in the existence of disturbance with wind speed in the good way and with the least variations.

In **Figure 13**, it can be found that the control effort or the adjustment of pitch angle is between of 14 and 22.5°. Due to changed areas of wind turbine efficiency, aim in this work is, regulating the power and speed of the generator at the nominal parameter in the third performance part. So, in this scenario by growing the value of wind to cut-out, the pitch angle has been improved, and this scenario leads to the decrease of power coefficient and the power is at its nominal value [4]. Furthermore, by reducing the speed of the wind, the blade pitch angle is decreased and at this step, to regulate the power and generator speed at nominal value, robust controller is designed. This controller attempts to control the pitch angle for accessing the high electric power and adjust the speed of generator about its nominal value. So, by applying this kind of controller, the control effort remains fewer than 25°, that is the utmost pitch angle of the wind turbine, stays bounded in the third area.

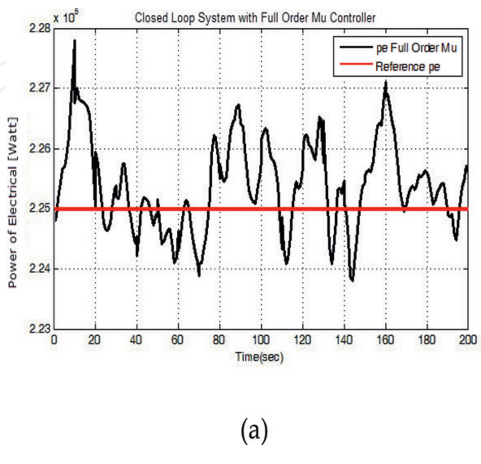

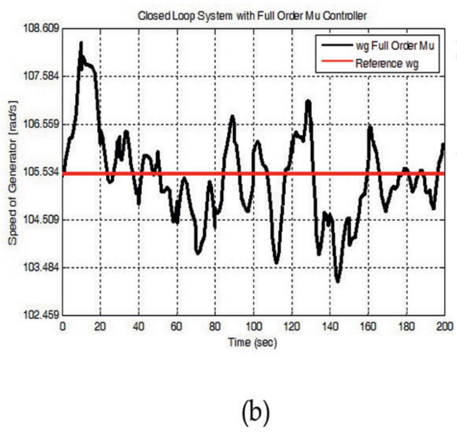

Figure 12. (a) The response of electric power produced by wind turbines to track input reference electrical power using μ controller. (b) The response of speed of the wind turbine generator to track input reference speed of generator using μ controller.

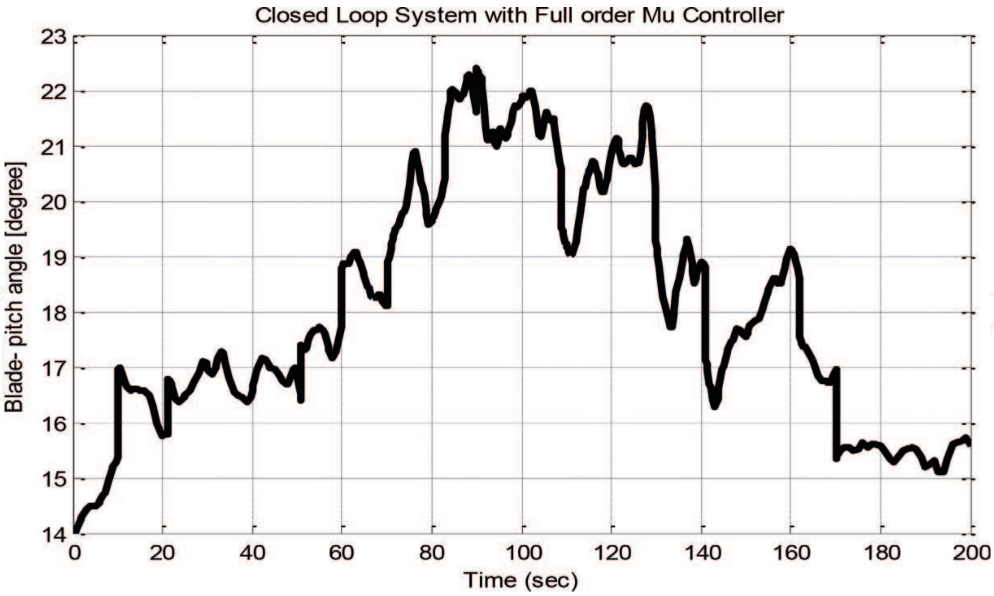

Figure 13. Pitch angle adjustment using the μ controller.

5. Conclusion

This work wanted to control the pitch angle of the wind turbine to regulate the speed of the wind turbine generator in the third area of procedure. In the third area, the generator speed, and electrical power are fix in their nominal parameter, and do constant. The existence of noise and disturbance in the model of wind are the main reason for high error rate in the generation of electrical power and generators' speed. Therefore, this paper suggested that the generation of electrical power and adjustment of the generator speed are practical if robust controller is employed and current errors (uncertainties) in the wind turbine system are taken into account. In most previous works have done, spring constant, damping coefficient and insignificant deviations of the linearization process are listed as uncertainties. These uncertainties are deemed to be true in appropriate weather conditions. Although, cold climate leads the turbine blades to freeze that is followed by mass growth. This mass development results in the decrease of electrical power generation, incorrect model operation and wrong data sending. So, new uncertainties were employed to the system in order to work out the mentioned challenges. After employing these uncertainties, μ controller is presented. Minimal variation about the reference parameter and fewer control action for variation the blades' angle (to obtain optimal power and adjust the speed of the generator) needs the use of μ controller. To be more accurate, the μ controller is more justifiable system in terms of disturbance cancelation.

A. Appendix

The wind turbine that is considered in this paper has the following specifications:

Characteristic of Vestas V29 Wind turbine

Vestas V29 wind turbine characteristic	Value
Electrical power of generator	225 KW
Rotor diameter	29 m
Rotor RPM	41/30.8 RPM
Angular speed of rotor	4.29 rad/s
Angular speed of generator	105.6 rad/s
Frequency	50–60 Hz

Author details

Tahere Pourseif[1]*, Majid Taheri Andani[2], Hamed Pourgharibshahi[3], Hassan Zeynali[1] and Arash Shams[1]

*Address all correspondence to: t.pourseif@gmail.com

1 Department of Electrical Engineering, Shahid Beheshti University, Tehran, Iran

2 Department of Electrical Engineering, Tehran University, Tehran, Iran

3 Advanced Technology University, Kerman, Iran

References

[1] Hau E. Wind Turbines: Fundamental, Technologies, Application, Economics Handbook. 3rd ed; 2013

[2] Blaabjerg F, Ma Ke. Future on power electronics for wind turbine systems. IEEE Journal of Emerging and Selected Topics in Power Electronics. 2013;**1**:139-152

[3] Kaldellis J, Zafirakis D. The wind energy revolution: A short review of a long history. Renewable Energy. 2011;**36**:1887-1901

[4] Bazilevs Y, Korobenko A, Deng X, Yan J. Novel structural modeling and mesh moving techniques for advanced fluid–structure interaction simulation of wind turbines. International Journal of Numerical Methods in Engineering. 2015;**102**:766-783

[5] Evangelista C, Valenciaga F, Puleston P. Active and reactive power control for wind turbine based on a MIMI 2-sliding mode algorithm with variable gains. IEEE Transactions on Energy Conversion. 2013;**28**:682-689

[6] Mirzaei M, Henrik H, Niemannand Kjolstad N. A μ ıt-synthesis approach to robust control of a wind turbine. In: Proceedings of 50th IEEE Conference on Decision and Control and European Control Conference, Orlando; 2011. pp. 645-650

[7] Mirzaei M, Henrik H, Niemannand Kjolstad N. DK-iteration robust control design of a wind turbine. In: IEEE International Conference on Control Applications Part of 2011 IEEE Multi-Conference on Systems and Control, Denver; 2011. pp. 1493-1498

[8] Etemaddar M, Hansen MOL, Moan T. Wind turbine aerodynamic response under atmospheric icing conditions. Journal of Wind Energy. 2014;**17**:241-265

[9] Shajiee S, Pao LY, Wagner PN, Moore ED, Mcleod RR. Direct ice sensing and localized closed-loop heating for active de-icing of wind turbine bladed. In: Proceedings of American Control Conference Washington; 2013. pp. 634-639

[10] Sunden B, Wu Z. On icing and icing mitigation of wind turbine blades in cold climate. Journal of Energy Resources Technology. 2015;**137**:1-10

[11] Jafarnejadsani H, Pieper J. Gain- Scheduled l_1-optimal control of variable-speed-variable-pitch wind turbines. IEEE Transactions on Control Systems Technology. 2015;**23**:372-379

[12] Iyasere E, Salah M, Dawson D, Wagner J, Tatlicioglu E. Optimum seeking-based nonlinear controller to maximise energy capture in a variable speed wind turbine. IET Control Theory and Applications. 2012;**6**:526-532

[13] Thomsen SC. Nonlinear control of wind turbine [Master thesis]; 2007

[14] Tang X, Deng W, Qi Z. Investigation of the dynamic stability of microgrid. IEEE Transactions on Power Systems. 2014;**29**:698-706

[15] Girsang IP, Dhupia JS, Muljadi E, Singh M, Pao LY. Gearbox and drivetrain models to study dynamic effects of modern wind turbines. IEEE Transactions on Industry Applications. 2014;**50**:3777-3786

[16] Shahriar MR, Borghesani P, Tan ACC. Speed-based diagnostics of aerodynamic and mass imbalance in large wind turbines. In: Proceedings of IEEE International Conference on Advanced Intelligent Mechtronics; 2015. pp. 796-801

[17] Habibi H, Cheng L, Zhang H, Kappatos V, Selcuk C, Gan T-H. A dual de-icing system for wind turbine blades combining high-power ultrasonic guided waves and low-frequency forced vibrations. Renewable Energy. 2015;**83**:859-870

[18] Gong X, Qiao W. Simulation ınvestigation of wind turbine ımbalance fault. In: Internation Conference on Power System Technology; 2010

[19] pourseif T, Afzalian A. Pitch angle control of wind turbine systems in cold weather conditions using mu robust controller. International Journal of Energy and Environmental Engineering, USA. March 2017;**8**(3):197-207

[20] Xiu-Xing Y, Yong-gang L, Wei L, Ya-jing G, Xiao-Jun W, Peng-fei L. Design, modeling and implementation of a novel pitch angle control system for wind turbine. Renewable Energy. 2015;**81**:599-608

[21] Lamraoui F, Fortin G, Benoit R, Perron J, Masson CH. Atmospheric icing impact on wind turbine production. International Journal of Cold Regions Science and Technology. 2014; **100**:36-49

[22] Pourseif T, Afzalian A. Design mu controller on wind turbine in cold weather conditions. In: The 4th International Conference on Control, Instrumentation and Automation (ICCIA), Qazvin, Iran; January 2016

[23] Skogestad S, Postlethwaite I. Multivariable Feedback Control Analysis and Design. John Wiley; 2013

IntechOpen